Single Carbon Nanotubes Probed by Photoluminescence Excitation Spectroscopy: The Role of Phonon-Assisted Transitions

H. Htoon, M. J. O'Connell, S. K. Doorn, and V. I. Klimov*

Chemistry Division, Los Alamos National Laboratory, Los Alamos, New Mexico 87545, USA
(Received 21 December 2004; published 1 April 2005)

We study light absorption mechanisms in semiconducting carbon nanotubes using low-temperature, single-nanotube photoluminescence excitation spectroscopy. In addition to purely electronic transitions, we observe several strong phonon-assisted bands due to excitation of one or more phonon modes together with the first electronic state. In contrast with a small width of emission lines (sub-meV to a few meV), most of the photoluminescence excitation features have significant linewidths of tens of meV. All of these observations indicate very strong electron-phonon coupling that allows efficient excitation of electronic states via phonon-assisted processes and leads to ultrafast intraband relaxation due to inelastic electron-phonon scattering.

The development of methods for producing luminescent samples of single-walled carbon nanotubes (NTs) [1,2], followed by intensive studies utilizing photoluminescence (PL) based spectroscopic techniques, have led to significant advances in the understanding of nanotube electronic structures [3–8]. Specifically, the use of PL excitation (PLE) spectroscopy allowed the mapping of spectral positions of ground-state and excited-state transitions for more than 30 NT species of different chiralities [3]. Single-NT PL studies [4,5] further revealed fine heterogeneities within nominally "single-species" NT ensembles associated with structural or chemical defects and fluctuations in the local environment. Low-temperature single-NT PL studies also indicated the importance of unintentional doping that could strongly affect NT optical spectra via the Fermi-edge singularity effect [5].

Despite this recent progress, the fundamental physics of NT interactions with light remains poorly understood. Some open questions include the role of excitonic effects in NT optical spectra [9–14], the branching between radiative and nonradiative decay channels [15–17], the role of phonons in light absorption or emission process [18], and the mechanisms for broadening of optical transitions. A significant difficulty in addressing these issues via traditional spectroscopic techniques arises from a large heterogeneity in available NT samples that contain a variety of NTs of different chiralities, lengths, doping levels, etc. These heterogeneities severely complicate an extraction of electronic structures of NTs of specific species from ensemble optical spectra. To overcome the problem of ensemble averaging, here we perform for the first time low-temperature single-NT PLE studies. This approach allows us to detect the structure of "absorbing" transitions in nanotubes of several different chiralities. One interesting observation is the large intensity of phonon-assisted transitions (phonon replicas) associated with the excitation of the ground electronic state simultaneously with one or more NT phonons. For NTs of relatively large diameters

(emitting at wavelengths longer than 1.1 μm), we resolve a PLE feature that is due to a direct excitation of the second electronic transition. Surprisingly, the intensity of the phonon replicas is comparable to this purely electronic feature, indicating strong electron-phonon coupling that facilitates second- and higher-order, phonon-assisted processes. In contrast to relatively narrow single-NT emission linewidths [5], single-NT PLE features are characterized by significant broadening of >35 meV. This observation indicates extremely fast relaxation of electronic excitations (< 20 fs), which provides an additional piece of evidence for a significant strength of electron-phonon interactions. Overall, the results of our single-NT PLE studies suggest that strong electron-phonon coupling results in a significantly more complex structure of NT absorption spectra than is assumed in a simple picture of optical transitions dominated by singularities in the one-dimensional (1D) energy spectrum.

In our studies, we use dilute submonolayers of micelle wrapped nanotubes [1] prepared on crystalline quartz substrates by drop casting from aqueous solutions. The samples contain short (average length ~200 nm) NTs of various chiralities. A conventional micro-PL setup is used to collect the emission of individual nanotubes [5]. The samples are excited by a continuous-wave Ti:sapphire laser tunable from 772 to 900 nm. To study nanotubes of small diameters emitting at wavelengths shorter than 1 μm, we use a liquid-nitrogen cooled charge coupled device, which allows us to obtain both spatially and spectrally resolved images of multiple nanotubes located along a vertical slit of a spectrometer. An example of such an image is presented in Fig. 1(a). Short horizontal line segments in this image represent the emission spectra of individual nanotubes. In PLE studies, we record spectrally resolved images of the sample projected along a spectrometer slit for each excitation wavelength. Then, we take a horizontal, ~10 μm wide "slice" of the image centered around a selected nanotube and integrate the PL intensity over the

vertical coordinate for each emission wavelength. The integrated signal is finally plotted as a function of excitation (vertical axis) and emission (horizontal axis) wavelengths to create the 2D plots shown in Fig. 1(b). To study large-diameter nanotubes with emission wavelength longer than 1 μm, we use a liquid-nitrogen-cooled, InGaAs, linear diode array detector that allows spectroscopic measurements but without providing imaging capabilities [top panels in Fig. 1(c) and 1(d)]. 2D plots similar to Fig. 1(b) were constructed by directly using PL spectra recorded for different excitation wavelengths [Fig. 1(c) and 1(d)] (see Ref. [19] for experimental details).

As reported in our earlier work [5], PL spectra of individual single-walled NTs are characterized by a wide distribution of positions, widths, and shapes. Specifically, we observed that large PL linewidths (> 6 meV) typically correlated with significant spectral asymmetry, which was explained in terms of the Fermi-edge singularity effect in unintentionally doped nanotubes. In this work, we concentrate on species that produce narrow (< 6 meV) symmetric emission spectra, which presumably indicates that these NTs do not have a significant level of doping. Such an approach allows us to eliminate at least one source of "nonintrinsic" heterogeneities, which simplifies the analysis of experimental results.

In the 2D plots of Fig. 1, PLE spectra of individual NTs appear as vertical line segments. However, in addition to such vertical lines, the 2D PLE plots also exhibit structures represented by diagonal lines. For these structures, the emission wavelength is separated from the excitation wavelength by a fixed energy interval, which is a signature of the Raman scattering process. As indicated in Fig. 1, most of the diagonal lines can be assigned to well-known

vibrational modes that were observed in previous Raman scattering studies of NTs [20,21].

One interesting observation is that the absorption shows a significant enhancement at the positions where the diagonal Raman lines cross the vertical PLE spectra. Such enhancement can, in principle, occur due to an enhancement of the intensity of the Raman signal in the presence of the resonant electronic state (resonant Raman scattering) and/or due to a PLE feature associated with a phonon-assisted transition involving a mode corresponding to a given diagonal line. Since Raman lines are characterized by a significantly narrower linewidth than electronic transitions, we can extract the PLE related contribution by performing a straightforward line-shape analysis [19].

The extracted, "Raman-free" PLE spectra of small (emission wavelength $\lambda_{em} < 1.1$ μm) and large ($\lambda_{em} > 1.1$ μm) diameter NTs are displayed in Fig. 2(a)−2(f) and Fig. 2(g)−2(l), respectively. These spectra exhibit several well-defined absorption bands associated with different phonon-assisted transitions. The most prominent phonon replica can be attributed to the excitation of the G band [the yellow region and blue bars in Fig. 2(a)−2(f)] and radial breathing mode (RBM) [red bars of Fig. 2(a) and 2(b)] phonons. In addition to single-phonon replicas, PLE spectra show features that can be interpreted in terms of simultaneous excitation of two different phonons. For example, the spectra in Fig. 2(b)−2(f) exhibit a feature at the position of the double-phonon replica associated with the G band and RBM phonons (red dotted bar). We also observe a replica associated with a G'-band mode [dotted green bars in Fig. 2(d)−2(g)], which corresponds to the simultaneous excitation of two disorder-related phonons. For large-diameter nanotubes, we even detect a triple-
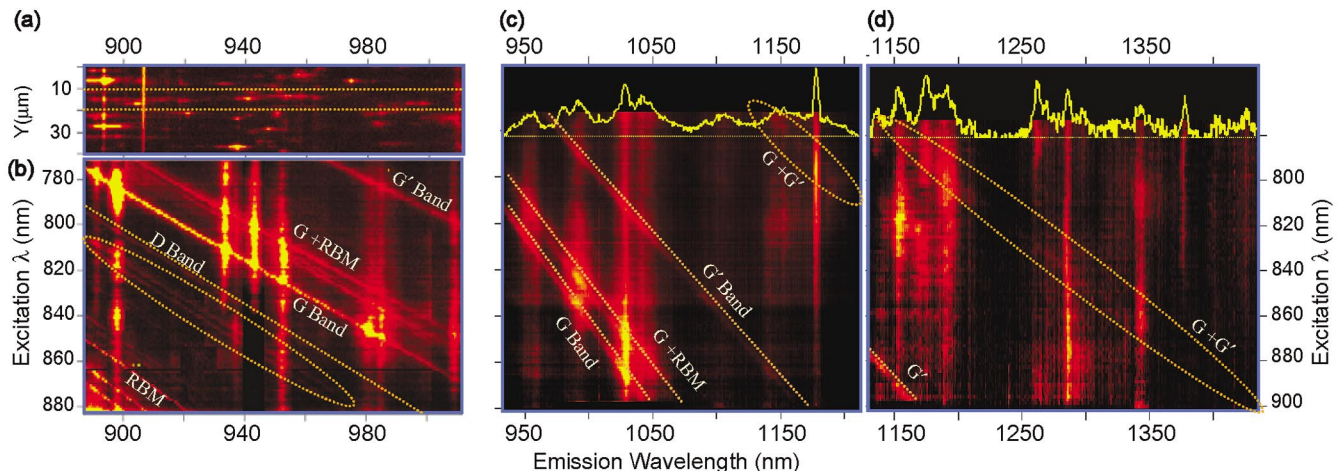

FIG. 1 (color).   (a) Spectrally dispersed image of NTs recorded at 4 K. Bright horizontal line fragments represent the emission spectra of individual nanotubes. Vertical displacement (y) of these lines is determined by the position of the tubes along the entrance slit of the spectrometer. (b) "Color-scale" representation of PL intensity as a function of excitation and emission wavelengths for the region marked in (a) by two dotted lines. (c), (d) The emission spectra taken with an InGaAs diode array detector (upper panel) and a two-dimensional color-scale plot created by stacking multiple spectra taken at different excitation wavelengths. In 2D images in panels (b), (c), and (d), vertical lines represent the PLE spectra of individual nanotubes, while diagonal lines are due to Raman scattering.

phonon replica $(G + G')$ that corresponds to simultaneous excitation of one G-band phonon and two disorder-induced phonons [brown dotted bar in Fig. 2(g)–2(k)]. Spectral positions and widths of phonon replicas derived from single-NT PLE spectra are schematically shown by green regions in Fig. 3, while single-phonon and multiphonon transitions responsible for these replicas are shown by blue solid and dotted lines (the latter are derived from the "diagonal" Raman spectra).

In addition to the PLE features associated with well-characterized Raman modes, we observe a PLE band associated with a group of weak Raman lines (combination modes) that appear above the RBM phonon replica, Refs. [20–23] [see the region marked by the dotted line in Fig. 1(a) and the green region in Fig. 2]. While the width and the intensity of this PLE feature varies widely from tube to tube, it is consistently observed in most of the individual NTs that we studied. Our results indicate that while these modes are not pronounced in Raman spectra, they strongly couple to electronic excitations and the corresponding phonon-assisted transitions represent an important mechanism for generation of electronic excitations.

Among the diagonal Raman lines we also observe a weak disorder-related D band $(\sim 1300 \text{ cm}^{-1})$. However, we do not detect a corresponding phonon replica in PLE spectra, while we clearly resolved the G'-band related phonon replica, which is due to simultaneous excitation

of two D-band phonons. The latter observation is consistent with results of previous Raman studies that indicate that the G' band is typically more intense than the D-band [24].

Our previous single-NT, low-temperature PL study indicates that the intrinsic linewidth of the lowest, ground-state transition in undoped NTs is quite small (~ 0.2 to ~ 6 meV) and nearly temperature independent up to 60 K [5]. These narrow linewidths were explained in terms of the one-dimensional (1D) excitonic nature of electronic excitations in nanotubes. Despite a continuous energy spectrum arising from the translational 1D motion (characterized by the translational momentum k), exciton emission lines are quite narrow because the momentum conservation only allows radiative recombination for a small portion of k vectors near the Brillouin zone center. In the case of phonon-assisted absorption processes this restriction is lifted (for the excitons with large-k vectors the momentum conservation can be satisfied due to the participation of the large-k vector phonons), which can lead to a significant broadening of corresponding spectroscopic features induced by exciton energy dispersion. This effect is likely responsible for a large width of the most of the PLE phonon replicas (linewidths up to 50 meV). In some cases, however, we detect narrow PLE peaks with linewidths of a few meV [see, e.g., spectra in Fig. 2(a) and 2(b)]. These sharp features may originate from the phonon-assisted transitions involving exciton states localized at impurities or defects. Such localized, 0D excitons are dispersion-free and, therefore, produce narrow, atomiclike absorption features.

As was pointed out earlier, for large-diameter nanotubes emitting in the range of wavelengths > 1.1 μm [Fig. 2(g)–
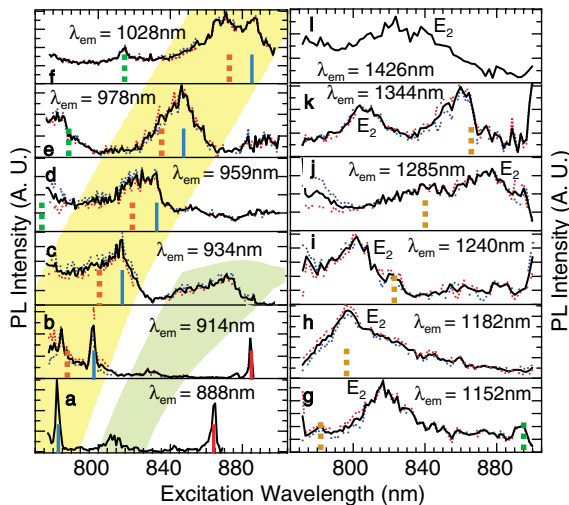

FIG. 2 (color). "Raman-free" PLE spectra of 12 individual nanotubes emitting in the range 870 to 1050 nm (a–f) and 1100 to 1430 nm (g–l). The blue and red dotted lines are two different scans, while the black line is the average. A good correspondence between two different scans indicates that the NTs selected for these measurements do not show significant fluctuations in the PL spectra due to blinking, line wondering, and/or photobleaching. Red and blue solid bars and red, green and brown dotted bars mark the positions of RBM, G,G + RBM, G', and $G + G'$ Raman modes, respectively. The emission wavelengths of individual NTs (λ_{em}) under investigation are shown in the figure.
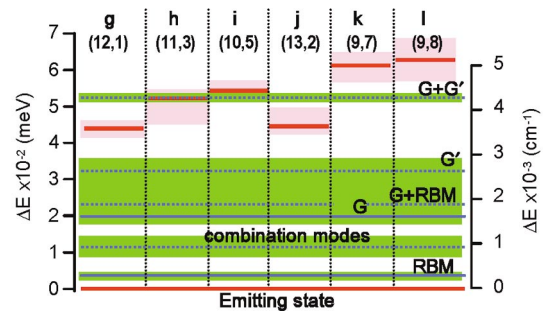

FIG. 3 (color). Energy diagram of optical transitions observed in PLE spectra (shown relative to the lowest emitting transition, which corresponds to zero energy). "Potential" positions of phonon replicas of the lowest transition associated with individual Raman modes (RBM and G) and the higher-order mode combinations (G + RBM, G', and $G + G'$) are shown by solid and dotted blue lines, respectively. The intense phonon-assisted PLE bands are shown as green regions. The positions and widths of high-energy purely electronic transitions observed for six different nanotubes shown in Fig. 2 are marked by the red lines and the pink regions. The tentative assignment of the (n,m) indices are indicated in the figure.

2(l)], we are able to detect high-energy PLE features (marked as E_2) that do not correlate with any of the Raman lines and, therefore, are likely due to direct excitation of the second electronic transition. The positions of these PLE features are shown by red bars in the energy diagram in Fig. 3, while their widths are schematically represented by pink regions. By comparing the energies of emission lines (E_1) and PLE "electronic" bands (E_2) to the energies of the E_{11} and E_{22} transitions reported in Ref. [3], we can tentatively assign NTs under investigation to certain (n, m) chiral indices (indicated in Fig. 3) (see Ref. [19]).

Similar to the large linewidths observed for a majority of the phonon-assisted PLE features, the bands related to the direct excitation of the second electronic transition are also characterized by significant broadening of 35 to 70 meV. This large line broadening indicates very fast dephasing of excited states with a characteristic time constant shorter than 20 fs. Since dephasing observed for the ground-state transition is significantly slower (> 100 fs; estimated from the PL linewidth of <6 meV), the latter result indicates very large intraband energy relaxation rates, likely resulting from highly efficient inelastic electron-phonon scattering.

Furthermore, we observe that the resonance between the E_2 transition and the $(G + G')$ replica produces a very large width (~ 70 meV) of the second electronic transition [Fig. 2(h)] compared with the off-resonant situation (linewidth of ~ 35 meV) [Fig. 2(g) and 2(i)]. This increase in the broadening can be explained by an increased relaxation rate resulting from highly efficient resonant emission of multiple phonons. The high efficiency of multiphonon processes is also indicated by the fact that the bands associated with two- and three-phonon transitions can be as intense as purely electronic features as illustrated by spectra in Fig. 3(k) and 3(j), in which we can resolve the E_2 feature simultaneously with the three-phonon $(G + G')$ replica [25].

In conclusion, we perform studies of mechanisms for light absorption in NTs by utilizing single-NT PLE spectroscopy. One important result of these studies is the observation of extremely strong electron-phonon coupling leading to a high intensity of phonon-assisted optical transitions and a large broadening of excited electronic states induced by inelastic electron-phonon scattering. Our observations of strong electron-phonon coupling and specifically a high efficiency of multiphonon processes indicate that electron-phonon interactions can in principle provide an efficient mechanism for nonradiative relaxation of the ground electronic state, which would explain very low efficiencies of nanotube emission typically observed in ensemble studies.

*Corresponding author.
Electronic address: klimov@lanl.gov

[1] M. J. O'Connell *et al.*, Science **297**, 593 (2002).
[2] J. Lefebvre, Y. Homma, and P. Finnie, Phys. Rev. Lett. **90**, 217401 (2003).
[3] S. M. Bachilo *et al.*, Science **298**, 2361 (2002).
[4] A. Hartschuh, H. N. Pedrosa, L. Novotny, and T. D. Krauss, Science **301**, 1354 (2003).
[5] H. Htoon, M. J. O'Connell, P. J. Cox, S. K. Doorn and V. I. Klimov, Phys. Rev. Lett. **93**, 027401 (2004).
[6] S. Zaric *et al.*, Science **304**, 1129 (2004).
[7] J. A. Misewich *et al.*, Science **300** 783 (2003); M. Freitag *et al.*, Phys. Rev. Lett. **93**, 076803 (2004).
[8] A. Hagen and T. Hertel, Nano Lett. **3**, 383 (2003).
[9] T. Ando, J. Phys. Soc. Jpn. **66**, 1066 (1997).
[10] C. L. Kane and E. J. Mele, Phys. Rev. Lett. **90**, 207401 (2003).
[11] E. Chang, G. Bussi, A. Ruini, and E. Molinari, Phys. Rev. Lett. **92**, 196401 (2004).
[12] C. D. Spataru, S. Ismail-Beigi, L. X. Benedict, and S. G. Louie, Phys. Rev. Lett. **92**, 077402 (2004).
[13] V. Perebeinos, J. Tersoff, and P. Avouris, Phys. Rev. Lett. **92**, 257402 (2004).
[14] O. J. Korovyanko *et al.*, Phys. Rev. Lett. **92**, 017403 (2004).
[15] F. Wang, G. Dukovic, L. E. Brus, and T. F. Heinz, Phys. Rev. Lett. **92**, 177401 (2004).
[16] G. N. Ostojic *et al.*, Phys. Rev. Lett. **92**, 117402 (2004).
[17] L. Huang, H. N. Pedrosa, and T. D. Krauss, Phys. Rev. Lett. **93**, 017403 (2004).
[18] V. Perebeinos, J. Tersoff, and P. Avouris, Phys. Rev. Lett. **94**, 027402 (2005).
[19] See EPAPS Document No. E-PRLTAO-94-061513 for the details of (1) low temperature, single-nanotube, photoluminescence excitation (PLE) experiment, (2) separation of "true" PLE signal from resonance-Raman signal, and (3) assignment of (n, m) chiral indices for large-diameter nanotubes. A direct link to this document may be found in the online article's HTML reference section. The document may also be reached via the EPAPS homepage (http://www.aip.org/pubserves/epaps.html) or from ftp.aip.org in the directory /epaps/. See the EPAPS homepage for more information.
[20] M. S. Dresselhaus and P. C. Eklund, Adv. Phys. **49**, 705 (2000).
[21] M. S. Dresselhaus *et al.*, Carbon **40**, 2043 (2002).
[22] A. M. Rao *et al.*, Science **275**, 187 (1997).
[23] C. Fantini *et al.*, Phys. Rev. Lett. **93**, 087401 (2004).
[24] R. Saito *et al.*, New J. Phys. **5**, 157 (2003).
[25] We would like to point out that the comparison of the intensities of the phonon replicas of the lowest transition and the high-energy PLE feature cannot be used as a direct measure of the electron-phonon coupling strength because of the possible existence of relaxation channels that remove carriers directly from the excited-state.